FINITE BEAM ELEMENT WITH PIEZOELECTRIC LAYERS AND FUNCTIONALLY GRADED MATERIAL OF CORE

Vladimír Kutiš[1], Justín Murín[1], Juraj Paulech[1], Juraj Hrabovský[1], Roman Gogola[1] and Jakub Jakubec[1]

[1]Department of Applied Mechanics and Mechatronics
Institute of Automotive Mechatronics
Faculty of Electrical Engineering and Information Technology
Slovak University of Technology in Bratislava
Ilkovičova 3, 812 19 Bratislava, Slovak Republic
e-mail: vladimir.kutis@stuba.sk, justin.murin@stuba.sk, juraj.paulech@stuba.sk,
juraj.hrabovsky@stuba.sk, roman.gogola@stuba.sk, jakub.jakubec@stuba.sk

Keywords: Piezoelectric Material, FGM, FEM, Beam Element, Transient Analysis

Abstract. *New smart materials have been developed in material science, that are suitable for mechatronic applications. Modern mechatronic systems are focusing on minimizing size, active control and low energy consumption. All this attributes can be incorporated into term Micro Electro Mechanical Systems (MEMS). To improve performance of MEMS system, new materials and technologies are developed - one of them, which found broad application usage is Functionally graded material (FGM). MEMS application usually contains multilayer structure and in some application class MEMS systems contain piezoelectric layers. Piezoelectric structures offer facilities to make motions. Piezoelectric layers can be also used to damp vibrations as an active damping or as an active sensor. For better understanding these multiphysical problems new mathematical models are developed.*

The paper deals with finite beam element with piezoelectric layers and functionally graded material of core. In the paper homogenization of FGM material properties and homogenization of core and piezoelectric layers is presented. In the process of homogenization direct integration method and multilayer method is used. There is also presented the derivation of individual submatrices of local stiffness and mass matrix, where concept of transfer constants is used. Functionality of new FGM finite beam with piezoelectric layers is presented by numerical experiments.

1 INTRODUCTION

New materials have been introduced in the area of mechanisms and mechatronic applications. Contemporary mechanical systems are focusing on minimizing size, active control and low energy consumption. All these attributes can be incorporated into term Micro Electro Mechanical System (MEMS). MEMS applications usually contain multilayer structure and some of these layers can have piezoelectric properties. Piezoelectric structures offer facilities to make motions or they can be used to damp vibrations as an active damper or as an active sensor.

2 PIEZOELECTRIC CONSTITUTIVE EQUATIONS

Piezoelectric constitutive equations describe the relationship between mechanical and electrical quantities [1]. This relationship is derived in tensor notation, but for practical usage it can be rewritten into matrices notation.

2.1 Tensor notation of piezoelectric constitutive equations

The form of the constitutive equations depends on chosen mechanical and electrical quantities and can be expressed in two basic configurations [2]. The first configuration is expressed by mechanical stress tensor components σ_{kl} and vector components of electric intensity E_k and has a form

$$D_i = \epsilon_{ik}^{\sigma} E_k + d_{ikl} \sigma_{kl} \tag{1}$$

$$\varepsilon_{ij} = d_{ijk} E_k + s_{ijkl}^{E} \sigma_{kl} \tag{2}$$

where ε_{ij} are strain tensor components, D_i are components of electric displacement vector, d_{ikl} are tensor components of piezoelectric constants, ϵ_{ik}^{σ} are components of permittivity tensor under constant mechanical stress and s_{ijkl}^{E} are components of compliance tensor under constant electric intensity.

The constitutive equations can be also expressed by strain tensor components ε_{kl} and vector components of electric intensity E_k and has a form

$$\sigma_{ij} = c_{ijkl}^{E} \varepsilon_{kl} - e_{ijk} E_k \tag{3}$$

$$D_i = e_{ikl} \varepsilon_{kl} + \epsilon_{ik}^{\varepsilon} E_k \tag{4}$$

where new quantities are components of stiffness tensor under constant electric intensity c_{ijkl}^{E} and components of piezoelectric modulus tensor e_{ijk}.

2.2 Matrix notation of piezoelectric constitutive equations

If we use symmetric properties of individual tensor in constitutive tensor equations, we can rewrite constitutive equations into matrix notation [3]. Then equations (1) and (2) have a form

$$D_i = \epsilon_{ik}^{\sigma} E_k + d_{iq} \sigma_q \tag{5}$$

$$\varepsilon_p = d_{pk} E_k + s_{pq}^{E} \sigma_q \tag{6}$$

and equations (3) and (4) can be rewritten in the form

$$\sigma_p = c_{pq}^{E} \varepsilon_q - e_{pk} E_k \tag{7}$$

$$D_i = e_{iq} \varepsilon_q + \epsilon_{ik}^{\varepsilon} E_k \tag{8}$$

D_i and E_k are vectors with three components, σ_q and ε_q are vectors with six components, matrices s_{pq}^E and c_{pq}^E have dimension 6×6, matrices d_{iq} and e_{pk} have dimension 3×6 and matrix $\epsilon_{ik}^\varepsilon$ has dimension 3×3. Constitutive equations (5) and (6) written in a component form can be rewritten as

$$\boldsymbol{\varepsilon} = \mathbf{s}^E \boldsymbol{\sigma} + \mathbf{d}^T \mathbf{E} \tag{9}$$

$$\mathbf{D} = \mathbf{d}\boldsymbol{\sigma} + \boldsymbol{\epsilon}^\sigma \mathbf{E} \tag{10}$$

and equations (7) and (8) can be rewritten as

$$\boldsymbol{\sigma} = \mathbf{c}^E \boldsymbol{\varepsilon} - \mathbf{e}^T \mathbf{E} \tag{11}$$

$$\mathbf{D} = \mathbf{e}\boldsymbol{\varepsilon} + \boldsymbol{\epsilon}^\varepsilon \mathbf{E} \tag{12}$$

3   BASIC FEM EQUATIONS FOR PIEZOELECTRIC STRUCTURE

To obtain basic FEM equations for piezoelectric structure, the Hamilton's principle is used and can be expressed in the form

$$\int_{t_1}^{t_2} \left(\delta L + \delta W \right) dt = 0 \tag{13}$$

where L is Lagrangian, W is work of external mechanical and electrical forces and t_1 and t_2 defined considered time interval.
Lagrangian of piezoelectric structure is given by

$$\begin{aligned} L =& T - U + W_e = \\ =& \int_V \frac{1}{2}\rho \dot{\mathbf{u}}^T \dot{\mathbf{u}} dV - \int_V \frac{1}{2}\boldsymbol{\varepsilon}^T \boldsymbol{\sigma} dV + \int_V \frac{1}{2}\mathbf{E}^T \mathbf{D} dV \end{aligned} \tag{14}$$

where T is kinetic energy of structure, U is potential energy of structure and W_e is electric energy stored in piezoelectric material. In kinetic energy term $\dot{\mathbf{u}}$ represents velocity vector.
Virtual work of external mechanical and electrical forces can be expressed as

$$\delta W = \sum \left(\delta \mathbf{u}^T \mathbf{F} \right) - \sum \left(\delta \boldsymbol{\phi}^T \mathbf{Q} \right) \tag{15}$$

where $\mathbf{F}$ and $\mathbf{Q}$ represents discrete forces and electric charges, respectively and $\mathbf{u}$ and ϕ are displacement vector and scalar electric potential, respectively.
Equation (13) can be rewritten using (14) and (15)

$$\begin{aligned} \int_{t_1}^{t_2} \Bigg[& \delta \int_V \frac{1}{2}\rho \dot{\mathbf{u}}^T \dot{\mathbf{u}} dV - \delta \int_V \frac{1}{2}\boldsymbol{\varepsilon}^T \boldsymbol{\sigma} dV + \delta \int_V \frac{1}{2}\mathbf{E}^T \mathbf{D} dV + \\ & + \sum \left(\delta \mathbf{u}^T \mathbf{F} \right) - \sum \left(\delta \boldsymbol{\phi}^T \mathbf{Q} \right) \Bigg] dt = 0 \end{aligned} \tag{16}$$

After some manipulation and using constitutive equations (11) and (12) Hamilton's principle for piezoelectric system can be expressed in form

$$\begin{aligned} \int_{t_1}^{t_2} \Bigg[& - \int_V \rho \delta \mathbf{u}^T \ddot{\mathbf{u}} dV - \int_V \delta \boldsymbol{\varepsilon}^T \mathbf{c}^E \boldsymbol{\varepsilon} dV + \int_V \delta \boldsymbol{\varepsilon}^T \mathbf{e}^T \mathbf{E} dV + \int_V \delta \mathbf{E}^T \mathbf{e}\boldsymbol{\varepsilon} dV + \\ & + \int_V \delta \mathbf{E}^T \boldsymbol{\epsilon}^\varepsilon \mathbf{E} dV + \sum \left(\delta \mathbf{u}^T \mathbf{F} \right) - \sum \left(\delta \boldsymbol{\phi}^T \mathbf{Q} \right) \Bigg] dt = 0 \end{aligned} \tag{17}$$

Using shape functions ($\mathbf{N}_u$, $\mathbf{N}_\phi$), we can write relationship between displacement of point and nodal displacement of finite element and between scalar electric potential of point and nodal scalar electric potential of finite element

$$\mathbf{u} = \mathbf{N}_u \mathbf{u}^e \tag{18}$$

$$\boldsymbol{\phi} = \mathbf{N}_\phi \boldsymbol{\phi}^e \tag{19}$$

Relationship between components of strain and components of nodal displacements has form

$$\boldsymbol{\varepsilon} = \mathbf{B}_u \mathbf{u}^e \tag{20}$$

Similarly relationship between components of electric field intensity and components of nodal potential can be written as

$$\mathbf{E} = -\mathbf{B}_\phi \boldsymbol{\phi}^e \tag{21}$$

Virtual strain and virtual electric field intensity can be expressed as

$$\delta\boldsymbol{\varepsilon} = \mathbf{B}_u \delta\mathbf{u}^e \tag{22}$$

$$\delta\mathbf{E} = -\mathbf{B}_\phi \delta\boldsymbol{\phi}^e \tag{23}$$

Equation (17) can be modified using equations (18)-(23)

$$\int_{t_1}^{t_2} \delta(\mathbf{u}^e)^T \left[-\left(\int_{V^e} \mathbf{N}_u^T \rho \mathbf{N}_u dV \right) \ddot{\mathbf{u}}^e - \left(\int_{V^e} \mathbf{B}_u^T \mathbf{c}^E \mathbf{B}_u dV \right) \mathbf{u}^e - \right.$$
$$\left. -\left(\int_{V^e} \mathbf{B}_u^T \mathbf{e}^T \mathbf{B}_\phi dV \right) \boldsymbol{\phi}^e + \mathbf{N}_u^T \mathbf{F} \right] dt + \tag{24}$$
$$+ \int_{t_1}^{t_2} \delta(\boldsymbol{\phi}^e)^T \left[\left(-\int_{V^e} \mathbf{B}_\phi^T \mathbf{e} \mathbf{B}_u dV \right) \mathbf{u}^e + \left(\int_{V^e} \mathbf{B}_\phi^T \boldsymbol{\epsilon}^\varepsilon \mathbf{B}_\phi dV \right) \boldsymbol{\phi}^e - \mathbf{N}_\phi^T \mathbf{Q} \right] dt = 0$$

From equations (24) we obtain finite element equations for piezoelectric analysis

$$\begin{bmatrix} \mathbf{M}_{uu}^e & \mathbf{0} \\ \mathbf{0} & \mathbf{0} \end{bmatrix} \begin{bmatrix} \ddot{\mathbf{u}}^e \\ \ddot{\boldsymbol{\phi}}^e \end{bmatrix} + \begin{bmatrix} \mathbf{C}_{uu}^e & \mathbf{0} \\ \mathbf{0} & \mathbf{0} \end{bmatrix} \begin{bmatrix} \dot{\mathbf{u}}^e \\ \dot{\boldsymbol{\phi}}^e \end{bmatrix} + \begin{bmatrix} \mathbf{K}_{uu}^e & \mathbf{K}_{u\phi}^e \\ \mathbf{K}_{\phi u}^e & \mathbf{K}_{\phi\phi}^e \end{bmatrix} \begin{bmatrix} \mathbf{u}^e \\ \boldsymbol{\phi}^e \end{bmatrix} = \begin{bmatrix} \mathbf{F}^e \\ \mathbf{Q}^e \end{bmatrix} \tag{25}$$

where

$$\mathbf{M}_{uu}^e = \int_V \mathbf{N}_u^T \rho \mathbf{N}_u dV \tag{26}$$

$$\mathbf{K}_{uu}^e = \int_V \mathbf{B}_u^T \mathbf{c}^E \mathbf{B}_u dV \tag{27}$$

$$\mathbf{K}_{u\phi}^e = \int_V \mathbf{B}_u^T \mathbf{e}^T \mathbf{B}_\phi dV \tag{28}$$

$$\mathbf{K}_{\phi u}^e = \int_V \mathbf{B}_\phi^T \mathbf{e} \mathbf{B}_u dV \tag{29}$$

$$\mathbf{K}_{\phi\phi}^e = -\int_V \mathbf{B}_\phi^T \boldsymbol{\epsilon}^\varepsilon \mathbf{B}_\phi dV \tag{30}$$

$$\mathbf{F}^e = \mathbf{N}_u^T \mathbf{F} \tag{31}$$

$$\mathbf{Q}^e = -\mathbf{N}_\phi^T \mathbf{Q} \tag{32}$$

4 FEM EQUATIONS OF FGM BEAM WITH PIEZOELECTRIC LAYERS

2D beam element with piezoelectric layers, where beam core is made from functionally graded material is shown in Figure 1, where all degrees of freedom are depicted. Mechanical degrees of freedom in each node are two displacements (in direction x a y) and rotation (in plane $x - y$) [6]. Electric degrees of freedom are electric potentials ϕ_i on 4 electrodes. The height of beam core made from FGM is h, the height of piezoelectric layer is h_p, the depth and the length of the beam element are b and L, respectively.

Material properties of FGM core are function of longitudinal and transversal coordinate x and y, material properties of piezoelectric layers are constants.
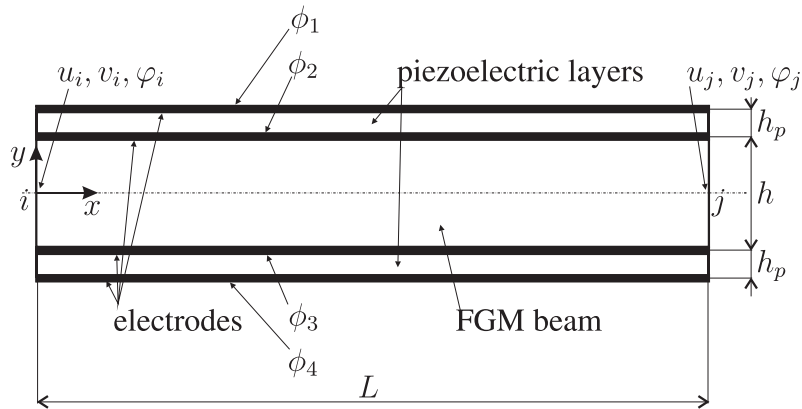
Figure 1: Electric DOF in 2D beam element

In order to derive individual submatrices of the beam element with piezoelectric layers and FGM core, two steps in homogenization process have to be performed. At first, homogenization of material properties of FGM core have to be performed, where direct integration method is used [6]. In the next step, homogenization of piezoelectric layers and homogenized FGM core (from step one) is performed. After these two operations, homogenized material properties of the beam vary through the length of the beam as a function of longitudinal coordinate x and are constant in transversal direction.

4.1 Equations for structural analysis

The structural submatrix $\mathbf{K}_{uu}^e$ for the beam element with piezoelectric layers can be expressed in a form

$$
\mathbf{K}_{uu}^e = \begin{bmatrix} k_u' & 0 & 0 & -k_u' & 0 & 0 \\ & k_{v2}' & k_{v3}' & 0 & -k_{v2}' & k_{v2} \\ \mathbf{S} & & k_{v33}' & 0 & -k_{v3}' & k_{v3} \\ & \mathbf{Y} & & k_u' & 0 & 0 \\ & & \mathbf{M} & & k_{v2}' & -k_{v2} \\ & & & & & k_{v23} \end{bmatrix} \tag{33}
$$

where individual components contain the influence of FGM core stiffness and also the influence of piezoelectric layers stiffness. The calculation of components is identical for classical multi-layer or FGM beam without piezoelectric layer and is described in [6]. Mass matrix $\mathbf{M}_{uu}^e$ can be calculated numerically using classical shape functions and homogenized density of FGM beam with piezoelectric layers according equation (26).

4.2 Equations for electric analysis

Electric field intensity in piezoelectric layer is constant and for top layer can by expressed as [4, 5]

$$E_1 = -\frac{\partial \phi}{\partial y} = \frac{\phi_2 - \phi_1}{h_p} \tag{34}$$

and for bottom layer as

$$E_2 = -\frac{\partial \phi}{\partial y} = \frac{\phi_4 - \phi_3}{h_p} \tag{35}$$

Both components of electric field intensity can be written in a form

$$\mathbf{E} = \begin{bmatrix} E_1 \\ E_2 \end{bmatrix} = - \begin{bmatrix} 1/h_p & -1/h_p & 0 & 0 \\ 0 & 0 & 1/h_p & -1/h_p \end{bmatrix} \begin{bmatrix} \phi_1 \\ \phi_2 \\ \phi_3 \\ \phi_4 \end{bmatrix} = -\mathbf{B}_\phi \boldsymbol{\phi}^e \tag{36}$$

For 1D problems the matrix of material properties for electric field – permittivity is reduced to only one material property ϵ^ε, but because the beam element contains two identical layers, we can write

$$\boldsymbol{\epsilon}^\varepsilon = \begin{bmatrix} \epsilon^\varepsilon & 0 \\ 0 & \epsilon^\varepsilon \end{bmatrix} \tag{37}$$

Then the equation (30) has a form

$$\mathbf{K}^e_{\phi\phi} = -\int_V \mathbf{B}_\phi^T \boldsymbol{\epsilon}^\varepsilon \mathbf{B}_\phi dV = -\int_L \mathbf{B}_\phi^T \boldsymbol{\epsilon}^\varepsilon \mathbf{B}_\phi A_p dx \tag{38}$$

where A_p is cross-section of one piezoelectric layer, i.e. $A_p = bh_p$.
After some mathematical manipulations the equation (38) can be expressed as

$$\mathbf{K}^e_{\phi\phi} = \begin{bmatrix} -\dfrac{A_p L \epsilon^\varepsilon}{h_p^2} & \dfrac{A_p L \epsilon^\varepsilon}{h_p^2} & 0 & 0 \\ \dfrac{A_p L \epsilon^\varepsilon}{h_p^2} & -\dfrac{A_p L \epsilon^\varepsilon}{h_p^2} & 0 & 0 \\ 0 & 0 & -\dfrac{A_p L \epsilon^\varepsilon}{h_p^2} & \dfrac{A_p L \epsilon^\varepsilon}{h_p^2} \\ 0 & 0 & \dfrac{A_p L \epsilon^\varepsilon}{h_p^2} & -\dfrac{A_p L \epsilon^\varepsilon}{h_p^2} \end{bmatrix} \tag{39}$$

4.3 Coupling of structural and electrical analysis

Piezoelectric material properties express coupling between mechanical and electrical field - matrices $\mathbf{e}$ or $\mathbf{d}$. The relationship between these two matrices can be expressed by elasticity matrix. In 1D problem in $x - y$ plane (in index notation $x_1 - x_2$) we have only one material property – e_{21} or d_{21}, where index 2 represents direction of piezoelectric layer polarization and also the direction of electric field intensity vector and index 1 defines direction of mechanical deformation. The relationship between these two quantities is reduced to expression $e_{21} = d_{21}E_p$ [7, 8], where E_p is Young modulus of elasticity of piezoelectric material. In reality, relationship between matrices $\mathbf{e}$ and $\mathbf{d}$ is more complicated and the quantity e_{21} computed from matrix $\mathbf{d}$ and elastic matrix for 3D system and the quantity e_{21} computed from d_{21} and E_p have

different values. Therefore if we have quantities e_{21} and d_{21} computed from matrix relationship, it is better to used them then simplified relationship.

Piezoelectric material properties of both piezoelectric layers are defined as

$$\mathbf{e} = \begin{bmatrix} e_{21} & 0 & -ye_{21} \\ e_{21} & 0 & -ye_{21} \end{bmatrix} \tag{40}$$

The expression $\mathbf{e}^T\mathbf{E}$ defines mechanical stress caused by piezoelectric effect. In the beam elements, internal quantities are not mechanical stress but internal forces and moments, then the first and the third column of matrix (40) multiplied by corresponding components of $\mathbf{B}_u$ and $\mathbf{B}_\phi$ as well as corresponding components of displacement $\mathbf{u}$ and potential ϕ represents axial forces and bending moments, respectively.

Description of piezoelectric behaviour by e_{21} is more suitable for sensor equation – matrix $\mathbf{K}^e_{\phi u}$, description by d_{21} is more suitable for actuator equation – matrix $\mathbf{K}^e_{u\phi}$, i.e.

$$\mathbf{e} = \begin{bmatrix} d_{21}E_p & 0 & -yd_{21}E_p \\ d_{21}E_p & 0 & -yd_{21}E_p \end{bmatrix} \tag{41}$$

Using equations (40) and (41) we can write (28) and (29) in form

$$\mathbf{K}^e_{u\phi} = \begin{bmatrix} -\dfrac{A_p d_{21} E_p}{h_p} & \dfrac{A_p d_{21} E_p}{h_p} & -\dfrac{A_p d_{21} E_p}{h_p} & \dfrac{A_p d_{21} E_p}{h_p} \\ 0 & 0 & 0 & 0 \\ \dfrac{A_y d_{21} E_p}{h_p} & -\dfrac{A_y d_{21} E_p}{h_p} & \dfrac{A_y d_{21} E_p}{h_p} & -\dfrac{A_y d_{21} E_p}{h_p} \\ \dfrac{A_p d_{21} E_p}{h_p} & -\dfrac{A_p d_{21} E_p}{h_p} & \dfrac{A_p d_{21} E_p}{h_p} & -\dfrac{A_p d_{21} E_p}{h_p} \\ 0 & 0 & 0 & 0 \\ -\dfrac{A_y d_{21} E_p}{h_p} & \dfrac{A_y d_{21} E_p}{h_p} & -\dfrac{A_y d_{21} E_p}{h_p} & \dfrac{A_y d_{21} E_p}{h_p} \end{bmatrix} \tag{42}$$

and

$$\mathbf{K}^e_{\phi u} = \begin{bmatrix} -\dfrac{A_p e_{21}}{h_p} & 0 & \dfrac{A_y e_{21}}{h_p} & \dfrac{A_p e_{21}}{h_p} & 0 & -\dfrac{A_y e_{21}}{h_p} \\ \dfrac{A_p e_{21}}{h_p} & 0 & -\dfrac{A_y e_{21}}{h_p} & -\dfrac{A_p e_{21}}{h_p} & 0 & \dfrac{A_y e_{21}}{h_p} \\ -\dfrac{A_p e_{21}}{h_p} & 0 & \dfrac{A_y e_{21}}{h_p} & \dfrac{A_p e_{21}}{h_p} & 0 & -\dfrac{A_y e_{21}}{h_p} \\ \dfrac{A_p e_{21}}{h_p} & 0 & -\dfrac{A_y e_{21}}{h_p} & -\dfrac{A_p e_{21}}{h_p} & 0 & \dfrac{A_y e_{21}}{h_p} \end{bmatrix} \tag{43}$$

where parameter A_y represents first moment of cross-section of piezoelectric layer

$$A_y = \frac{1}{2}A_p(h + h_p) \tag{44}$$

4.4 FEM equations for the beam element with piezoelectric layers

FEM equations for beam element with piezoelectric layers and FGM core for transient analysis have classical form

$$\begin{bmatrix} \mathbf{M}^e_{uu} & \mathbf{0} \\ \mathbf{0} & \mathbf{0} \end{bmatrix} \begin{bmatrix} \ddot{\mathbf{u}}^e \\ \ddot{\boldsymbol{\phi}}^e \end{bmatrix} + \begin{bmatrix} \mathbf{C}^e_{uu} & \mathbf{0} \\ \mathbf{0} & \mathbf{0} \end{bmatrix} \begin{bmatrix} \dot{\mathbf{u}}^e \\ \dot{\boldsymbol{\phi}}^e \end{bmatrix} + \begin{bmatrix} \mathbf{K}^e_{uu} & \mathbf{K}^e_{u\phi} \\ \mathbf{K}^e_{\phi u} & \mathbf{K}^e_{\phi\phi} \end{bmatrix} \begin{bmatrix} \mathbf{u}^e \\ \boldsymbol{\phi}^e \end{bmatrix} = \begin{bmatrix} \mathbf{F}^e \\ \mathbf{Q}^e \end{bmatrix} \tag{45}$$

where individual submatrices are defined by (33), (39), (42) and (43), vector of nodal unknowns is defined as

$$
\begin{bmatrix} \mathbf{u}^e \\ \boldsymbol{\phi}^e \end{bmatrix} = \begin{bmatrix} u_i & v_i & \varphi_i & u_j & v_j & \varphi_j & \phi_1 & \phi_2 & \phi_3 & \phi_4 \end{bmatrix}^T \tag{46}
$$

and vector of nodal loads is defined as

$$
\begin{bmatrix} \mathbf{F}^e \\ \mathbf{Q}^e \end{bmatrix} = \begin{bmatrix} F_{xi} & F_{yi} & M_i & F_{xj} & F_{yj} & M_j & Q_1 & Q_2 & Q_3 & Q_4 \end{bmatrix}^T \tag{47}
$$

where Q_1, Q_2, Q_3 and Q_4 are electric charge on electrodes 1, 2, 3 and 4, respectively.

5 NUMERICAL EXAMPLES

All derived equations for FGM beam with piezoelectric layers were implemented in our FEM code MultiFEM.
In this section three numerical examples are presented:

- Example 1 – considered simple beam is made from FGM with attached piezoelectric layers, only static analysis is considered

- Example 2 – the same simple beam as in Example 1 is considered, but analysis is transient

- Example 3 – considered structure contains three beam parts with partially attached piezo-electric layers, two beam parts are made from FGM and one beam part has constant material properties

5.1 Material properties of FGM structure and piezoelectric layers

In all three examples, the same functionally graded material is considered. Material of matrix (index m) is NiFe with constant density and Young's modulus and material of fibre (fibre – index f) is tungsten with constant density and Young's modulus:

- Young's modulus: $E_m = 255$ GPa, $E_f = 400$ GPa

- density: $\rho_m = 9200$ kg/m^3, $\rho_f = 19300$ kg/m^3

Volume fractions of both constituents $v_m(x, y)$ and $v_f(x, y)$ vary along the length (axis x) and height (axis y) of beams according equations:

$$
v_m(x,y) = -1.\overline{3} \times 10^8 x^3 y^2 + 1333.\overline{3}x^3 + 2. \times 10^7 x^2 y^2 - 200.x^2 - 40000.y^2 + 1. \quad [\text{-}] \tag{48}
$$
$$
v_f(x,y) = 1.\overline{3} \times 10^8 x^3 y^2 - 1333.\overline{3}x^3 - 2. \times 10^7 x^2 y^2 + 200.x^2 + 40000.y^2 \quad [\text{-}] \tag{49}
$$

Both functions of volume fractions for beam with length 0.1 m and height 0.01 m are shown in Figure 2.

Effective material properties of FGM are defined by material properties of constituents and their variations and Young's modulus and density of considered FGM have form

$$
\begin{aligned}
E_{\text{FGM}}(x,y) = &1.9\overline{3} \times 10^{19} x^3 y^2 - 1.9\overline{3} \times 10^{14} x^3 - 2.9 \times 10^{18} x^2 y^2 + \\
&+ 2.9 \times 10^{13} x^2 + 5.8 \times 10^{15} y^2 + 2.55 \times 10^{11} \quad [\text{Pa}]
\end{aligned} \tag{50}
$$

$$
\begin{aligned}
\rho_{\text{FGM}}(x,y) = &1.34667 \times 10^{12} x^3 y^2 - 1.34667 \times 10^7 x^3 - 2.02 \times 10^{11} x^2 y^2 + \\
&+ 2.02 \times 10^6 x^2 + 4.04 \times 10^8 y^2 + 9200. \quad [\text{kg/m}^3]
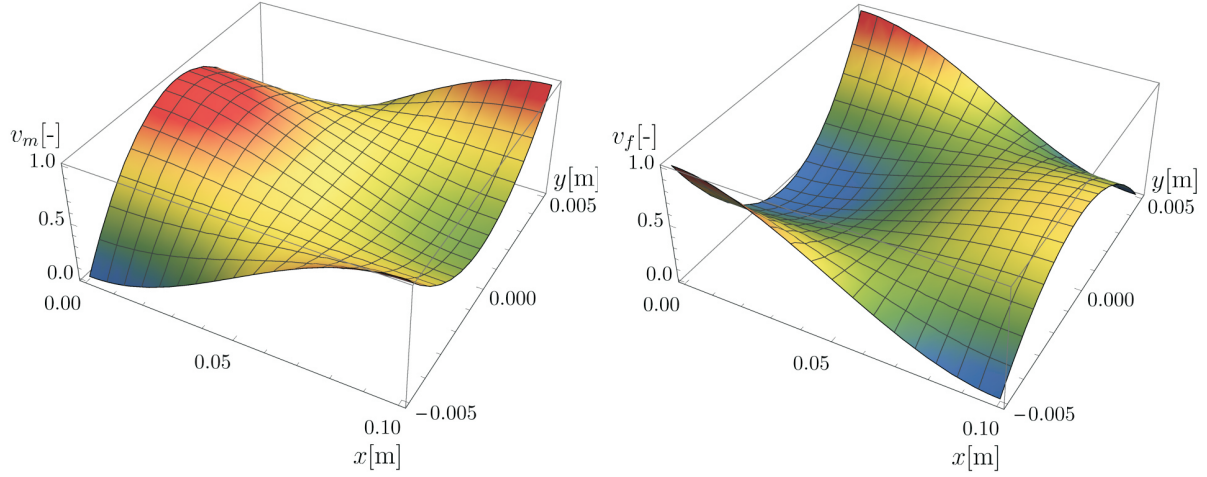\end{aligned} \tag{51}
$$

Figure 2: Left – volume fraction of matrix, right – volume fraction of fibre

In all three examples, height and depth of beam cross-section is 0.01m. Homogenized material properties of investigated FGM beams can be calculated by defined cross-section parameters of beams and by effective material properties and have following forms:

$$E_{\text{FGM}}^N(x) = -3.\overline{2} \times 10^{13}x^3 + 4.8\overline{3} \times 10^{12}x^2 + 3.0\overline{3} \times 10^{11} \quad \text{[Pa]} \tag{52}$$

$$E_{\text{FGM}}^M(x) = 9.\overline{6} \times 10^{13}x^3 - 1.45 \times 10^{13}x^2 + 3.42 \times 10^{11} \quad \text{[Pa]} \tag{53}$$

$$\rho_{\text{FGM}}(x) = -2.2\overline{4} \times 10^6 x^3 + 33666.\overline{6}x^2 + 12566.\overline{6} \quad \text{[kg/m}^3\text{]} \tag{54}$$

$E_{\text{FGM}}^N(x)$ and $E_{\text{FGM}}^M(x)$ represent homogenized Young's modulus for axial loading and for bending, respectively.

Piezoelectric layers in investigated beams are made from PZT5A piezoelectric material. PZT5A is orthotropic material and has following material properties (direction of poling has index 3):

- mechanical properties:

    - Young's moduli: $E_1 = 61$ GPa, $E_2 = 61$ GPa, $E_3 = 53,2$ GPa
    - Poisson numbers: $\mu_{12} = 0.35$, $\mu_{13} = 0.38$, $\mu_{23} = 0.38$
    - shear moduli: $G_{12} = 22.6$ GPa, $G_{13} = 21.1$ GPa, $G_{23} = 21.1$ GPa
    - density: 7750 kg/m^3

- piezoelectric properties: $d_{31} = -171 \times 10^{-12}$ C/N, $d_{33} = 374 \times 10^{-12}$ C/N, $d_{15} = 584 \times 10^{-12}$ C/N, $d_{24} = 584 \times 10^{-12}$ C/N

- relative permittivity: $\epsilon_{11}^\sigma = 1728.8$, $\epsilon_{22}^\sigma = 1728.8$, $\epsilon_{33}^\sigma = 1694.9$

5.2 Example 1 – static analysis of piezoelectric beam

Figure 3 shows simple cantilever made of FGM with piezoelectric layers, which is loaded by transversal force F at free end. Electrodes on top and bottom piezoelectric layers are short circuited. The goal of analysis is to investigate static responds of structure on prescribed loading and compare results of 1D model with results of 2D model.

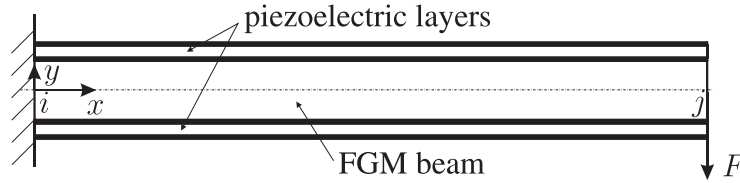Geometry parameters of beam are:

Figure 3: Example 1: static analysis of FGM beam with piezoelectric layers

- length 0.1 m

- height of FGM core 0.01 m, height of piezoelectric layer 0.001 m

- depth of beam 0.01 m

Material of beam:

- core of beam is made from FGM (NiFe-tungsten) and its effective and homogenized material properties are described by equations (50)-(54)

- piezoelectric layers are made from PZT5A – reduced properties $\overline{e}_{31} = \dfrac{d_{31}}{s_{11}^E} = -10.43$ C/m^2

Using multilayered method homogenized Young's modulus for axial loading and for bending and homogenized density of whole beam can be calculated using homogenized material properties of FGM core and constant material properties of piezoelectric layers and they have form

$$E^N(x) = -2.68519 \times 10^{13}x^3 + 4.02778 \times 10^{12}x^2 + 2.62944 \times 10^{11} \quad \text{[Pa]} \tag{55}$$

$$E^M(x) = 5.59414 \times 10^{13}x^3 - 8.3912 \times 10^{12}x^2 + 2.23616 \times 10^{11} \quad \text{[Pa]} \tag{56}$$

$$\rho(x) = -1.87037 \times 10^6 x^3 + 280556.x^2 + 11763.9 \quad \text{[kg/m}^3\text{]} \tag{57}$$

Boundary conditions:

- left end – fixed

- right end – transversal force $F = 10$ N

The static analysis of system was performed by new FGM beam element with piezoelectric layers. The analysis was performed by 1, 2, 4 and 10 elements – see Figure 4 left.

Deformed shape of beam is shown in Figure 4 right. Displacement in y direction of free end is -10.63×10^{-6} m. Electric charge on top electrodes for FEM models with different number of elements are summarized in Table 1.

The same problem was analyzed by FEM code ANSYS, where two types of plane elements were used – PLANE223 with piezoelectric capabilities and PLANE183. Because material properties of FGM core vary along the length and height of beam, discretized 2D model contains 6400 elements. Displacement in y direction of free end was -10.70×10^{-6} m and total electric charge on top electrode was 9.2715×10^{-8} C.

As we can see from obtained results, new FGM beam element with piezoelectric layers is very accurate and effective in static analysis, because variation of material properties of FGM core of beam is directly incorporated into stiffness matrix.
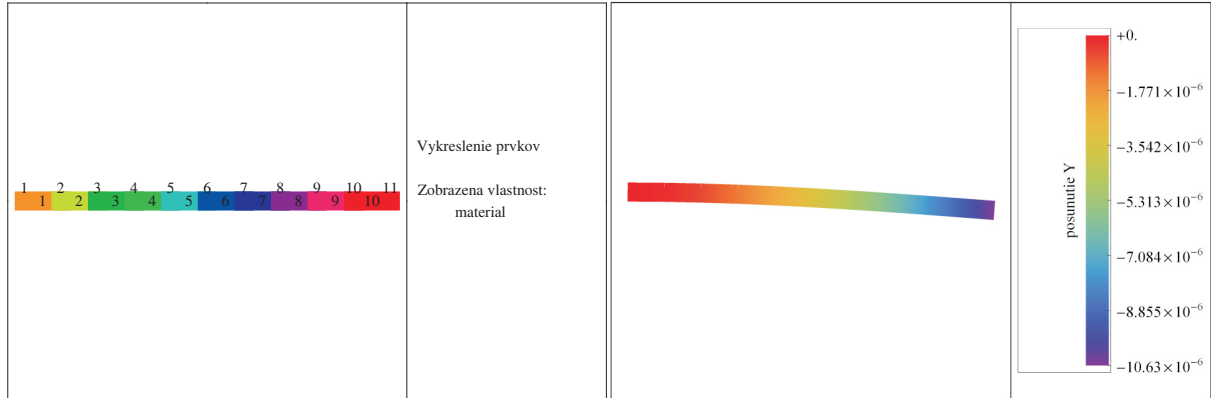
Figure 4: Example 1: left – discretized beam with node and element numbers, right – deformation of beam

Number of elements	1	2	4	10
$Q_{\text{elem 1}}$ [C]	9.2650×10^{-8}	6.8159×10^{-8}	3.9209×10^{-8}	1.6939×10^{-8}
$Q_{\text{elem 2}}$ [C]		2.4491×10^{-8}	2.8950×10^{-8}	1.5256×10^{-8}
$Q_{\text{elem 3}}$ [C]			1.8203×10^{-8}	1.3624×10^{-8}
$Q_{\text{elem 4}}$ [C]			6.2883×10^{-9}	1.1998×10^{-8}
$Q_{\text{elem 5}}$ [C]				1.0343×10^{-8}
$Q_{\text{elem 6}}$ [C]				8.6318×10^{-9}
$Q_{\text{elem 7}}$ [C]				6.8450×10^{-9}
$Q_{\text{elem 8}}$ [C]				4.9743×10^{-9}
$Q_{\text{elem 9}}$ [C]				3.0245×10^{-9}
$Q_{\text{elem 10}}$ [C]				1.0157×10^{-9}
Q_{SUM} [C]	9.2650×10^{-8}	9.2650×10^{-8}	9.2650×10^{-8}	9.2650×10^{-8}

Table 1: Example 1: Electric charge on individual electrodes

5.3 Example 2 – transient analysis of piezoelectric beam

In Example 2 transient analysis of FGM beam with piezoelectric layers with the same geometry and material parameters as in Example 1 was performed. Electrodes on top and bottom piezoelectric layers are short circuited. The goal of analysis is to investigate free vibration of structure without considering damping.
Boundary conditions:

- left end – fixed

- right end – free

Initial conditions:

- initial displacement of nodes – initial deformation of system is defined by prescribed displacement of free end in vertical direction +0.01m

- initial velocity of nodes – all nodes have zero initial velocities

The transient analysis of system was performed by new FGM beam element with piezoelectric layers. In the analysis Newmark integration scheme was used. Total simulation time was 5 ms

and number of equidistant substeps was 80. 1D model of system was discretized by 10 elements – see Figure. 4 left.

Displacement of nodes 4, 8 and 11 in direction y as function of time are shown in Figure 5 left. Time variations of electric charge in top electrode on elements 2 and 4 are shown in Figure 5 right.
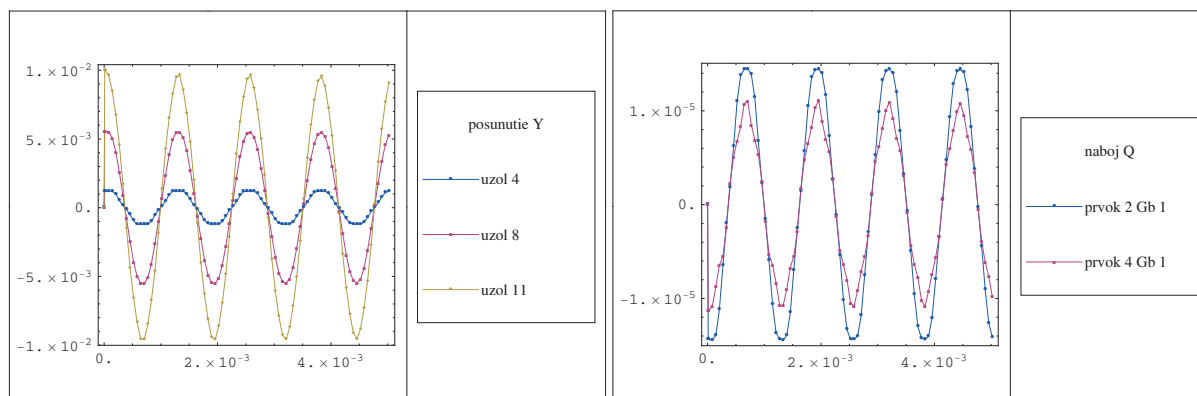

Figure 5: Example 2: left – Y displacement time variation of nodes (4, 8, 11), right – charge time variation of top electrodes on elements (2, 4)

5.4   Example 3 – transient analysis of simple structure

Figure 6 shows simple structure, which contains three beams. Piezoelectric layers are partially attached to the beam 1 and 2. Electrodes on top and bottom piezoelectric layers are short circuited. The goal of analysis is to investigate free vibration of structure with considering damping.
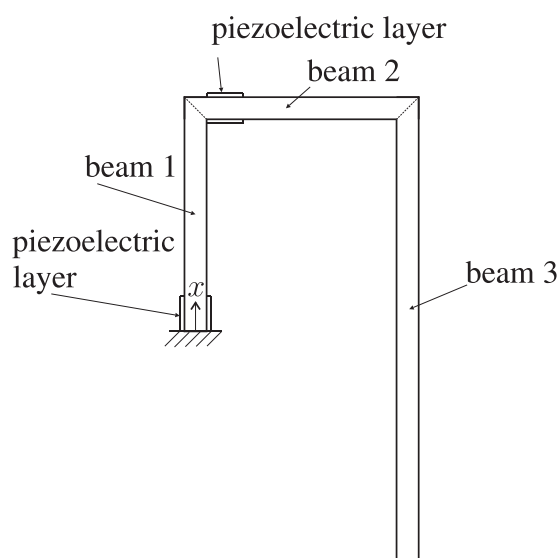

Figure 6: Example 3: free vibration of structure with piezoelectric elements

Geometry parameters of beams are:

- cross-section – all beams have height and depth of cross-section 0.01 m, height of piezo-electric layers is 0.001 m and its depth is 0.01 m

- length – beam 1 and 2 have length 0.05 m and beam 3 has length 0.1 m, length of piezo-electric layers is 0.01 m

Material parameters of beam are:

- core of beam – beam 1 and 2 are made from FGM, homogenized material properties are defined by equations (52)-(54), beam 3 has constant material properties: $E = 319.4$ GPa, $\rho = 13989.6$ kg/m^3

- piezoelectric layer – PZT5A

Three different types of beam finite elements were used in transient analysis of system: FGM beam element, FGM beam element with piezoelectric layers and beam element with Hermite shape functions. Discretized 1D model of system is shown in Figure 7, where nodes and element types are depicted.
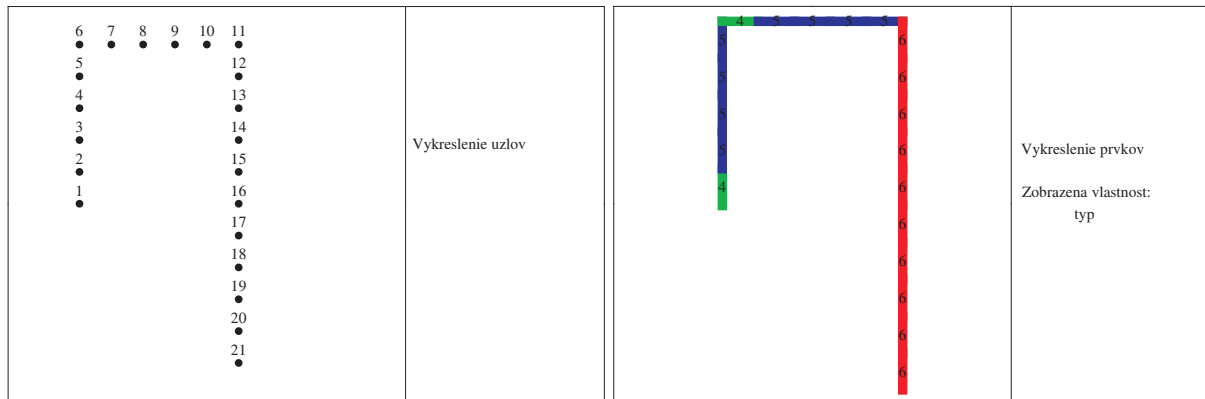

Figure 7: Example 3: left – nodes, right – elements with element types numbering

Boundary conditions:

- left end – fixed

- right end – free

Initial conditions:

- initial displacement of nodes – initial deformation of system is defined by prescribed displacement of free end in horizontal direction +0.01m

- initial velocity of nodes – all nodes have zero initial velocities

In the analysis Newmark integration scheme was used. Total simulation time was 7.5 ms and number of equidistant substeps was 400. In the analysis Rayleigh damping was used. Mass-proportional damping coefficient and stiffness-proportional damping coefficient had the same value 1×10^{-5}.

Deformed shape of system at the end of simulation time (7.5 ms) is shown in Figure 8 left. Figure 8 right shows time variation of electric charge in top electrode on elements 1 and 6. Displacements of nodes 8 and 21 as function of time in direction x and y are shown in Figure 9 left and right, respectively.
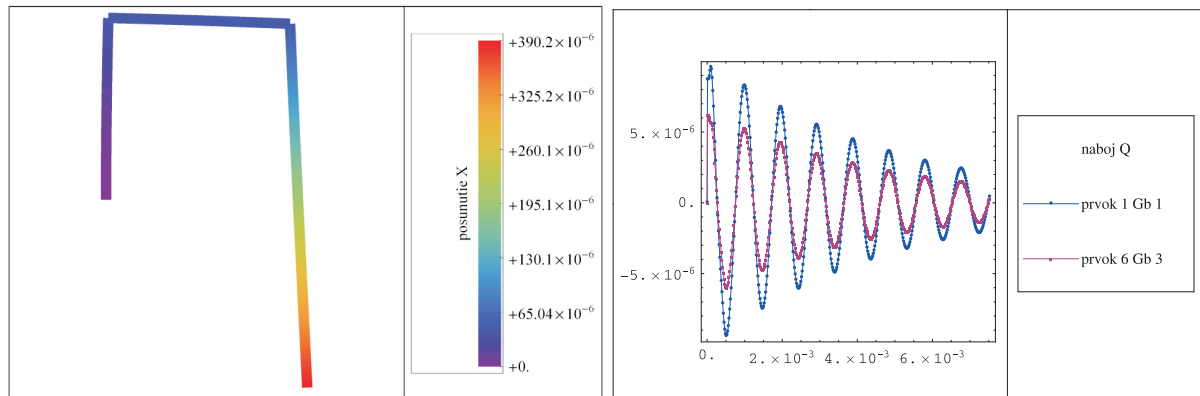
Figure 8: Example 3: left – X displacement of structure at time 7.5ms, right – charge time variation of top electrode on element 1 and 6
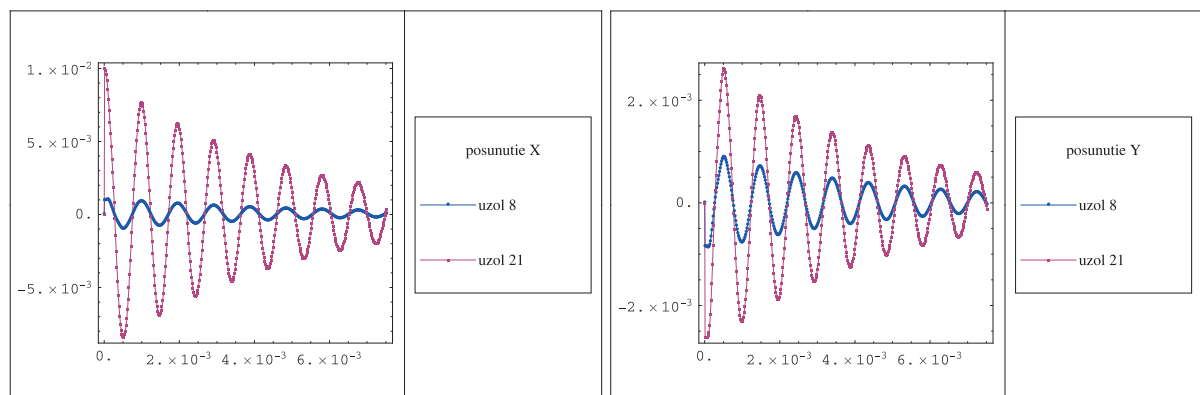

Figure 9: Example 3: left – X displacement time variation of nodes (8, 21), right – Y displacement time variation of nodes (8, 21)

6 CONCLUSIONS

The paper presents new beam finite element with piezoelectric layers, where core of the beam can be made of FGM materials. Such combination of materials is very attractive for mechatronic applications, because material composition of FGM core can be optimized for design stress state and deformation can be controlled by voltages on electrodes. The beam finite element can be used for analysis of such systems very effectively and accurately.

ACKNOWLEDGEMENT

REFERENCES

[1] Moheimani, S.O.R. and Fleming, A.J.. *Piezoelectric Transducers for Vibration Control and Damping*. Springer, (2006).

[2] Ballas, R.G. *Piezoelectric Multilayer Beam Bending Actuators*, Springer, (2007).

[3] Barnett, A.R., Peelamedu, S.M., Dukkipati, R.V. and Naganathan, N.G. Finite Element Approach to Model and Analyze Piezoelectric Actuators. *JSME International Journal*, (2001) **44**:476–485.

[4] I. Bruant, G. Coffignal, F. Lene, M. Verge. Active control of beam structures with piezo-electric actuators and sensors: modeling and simulation. *Smart Material Structures* (2001) **10**:404–408.

[5] Q. Luo, L. Tong. An accurate laminated element for piezoelectric smart beam including peel stress. *Computational Mechanics* (2004) **33**:108–120.

[6] Kutiš, V., Murín, J., Belák, R., Paulech, J. Beam element with spatial variation of material properties for multiphysics analysis of functionally graded materials. *Computers & Structures*, (2011) **89**:1192–1205.

[7] Preumont, A. *Mechatronics Dynamics of Electromechanical and Piezoelectric Systems*, Springer, (2006).

[8] Preumont, A. *Vibration Control of Active Structures*, Kluwer, (2002).